Finite-geometry effects, superfluid density, and universality in ^{3}He-^{4}He mixtures near the superfluid transition

W. C. Thomlinson,* G. G. Ihas,† and F. Pobell
Institut für Festkörperforschung Kernforschungsanlage, 517 Jülich, West Germany
(Received 20 January 1975)

The amplitude and velocity of second sound near T_λ have been measured in ^{3}He-^{4}He mixtures with molar ^{3}He concentrations $X = 0.000$, 0.096, 0.204, 0.396, and 0.555. The sound was generated and detected in resonators equipped with superleak transducers with channel sizes $d = 0.2$ μm and $d = 0.6$ μm. The onset temperatures $T_0(X)$ for superfluidity have been determined by observing the vanishing of the second-sound amplitude at temperatures below $T_\lambda(X)$. The reduced shift, $\epsilon_0 = 1 - T_0(X)/T_\lambda(X)$, of the onset temperature T_0 increases by about a factor of 6 for $X = 0$ to $X = 0.4$. The critical exponents in the equations $\epsilon_0 = (d/d^*)^{-\lambda'}$ and $l = l^*\epsilon^{-\nu'}$ are independent of X to within 3% (l is the onset length for superfluidity). In addition, the quantity $l\rho_s/T$ is found to be independent of concentration in agreement with theoretical predictions. For the superfluid fraction, $\rho_s/\rho = k\epsilon^\zeta$, we find that the exponent ζ is nearly concentration independent for $X = 0.0$ to 0.4, whereas the amplitude k decreases by almost an order of magnitude.

I. INTRODUCTION

The scaling theory of critical phenomena[1] and the concept of universality[2] have recently been substantially supported by explicit calculations of critical exponents.[3] The resulting theoretical predictions have been tested experimentally in a number of systems. The superfluid phase transition of pure ^{4}He has been used extensively in these studies through measurements of hydrodynamic and thermodynamic properties.[4,5] This system is popular because of its extremely high purity and homogeneity and the high precision to which its temperature and pressure may be regulated. It has been found that the critical exponents for the superfluid fraction ρ_s/ρ,[6] and of the coherence length ξ are universal (unaffected by pressure).[7] In addition, the apparent contradictions to the universality concept by the behavior of the specific heat C_P as a function of pressure[8] has been very recently removed by a detailed study of the isobaric thermal expansion coefficient.[9] Furthermore, the quantity $\rho_s\xi/T$ is found to be constant, independent of pressure and temperature,[7] as expected from theory.[10,11]

Since the concentration X of ^{3}He in ^{4}He is also an inert variable for the λ transition (that is, it affects neither the dimensionality of the system nor the number of degrees of freedom of its order parameter), one may perform the same tests in mixtures of ^{3}He in ^{4}He.[4,5] Several laboratories have measured the superfluid fraction ρ_s/ρ as a function of temperature and concentration by measuring the velocity u_2 of second sound.[12-17] The data have been analyzed using Khalatnikov's two-fluid equations for mixtures.[18,19] The resulting data showed unexpected results; namely, a strongly concentration-dependent critical exponent ζ for the superfluid fraction ($\rho_s/\rho = k\epsilon^\zeta$ where $\epsilon = 1 - T/T_\lambda$). In addition to measuring u_2 we measured the onset temperature $T_0(X)$ for superfluidity in ^{3}He-^{4}He mixtures by observing the vanishing of second-sound signals in resonators equipped with superleak transducers.[7,14] In order for vibrating filter membranes to generate or detect second sound, the onset length l for superfluidity. When the tem- the onset length for superfluidity. When the temperature is raised the onset length increases and eventually becomes comparable to the channel diameter. Then, superfluidity vanishes in the channels, and the filter membranes are not suitable for the production or detection of second sound. This type of measurement gave the critical exponent λ' describing the dependence of the onset temperature on the channel geometry, $\epsilon_0 = (d/d^*)^{-\lambda'}$.[20] The exponent λ' is related by a scaling argument to the correlation length exponent ν' via the relation $\nu' = 1/\lambda'$. In addition, we calculated the quantity $\rho_s l/T$ from our data.

The results presented in our announcing letter[14] on this work indicate the confusion that this subject was in at the time of their publication. It was generally agreed that for the mixtures the superfluid exponent ζ deduced from the data for the second-sound velocity lacked universality[12,14] and that its prefactor k changed an exceptionally large amount with changing concentration.[12,14,21] However, our measurements of the onset temperature showed that λ' (to which ν' and ζ are believed to be related by scaling) was universal.[14] This

seemed paradoxical. In addition, combining the two sets of data to form $\rho_s l/T$ indicated that the predicted constancy of this quantity, which is fulfilled so well in ^{4}He, failed when only a few percent of ^{3}He were added.[14]

These contradictions led Ahlers to the discovery of a widely propagating error in the usage of the Khalatnikov theory needed to obtain ρ_s/ρ from u_2.[22] This error consisted of using the entropy S instead of $S[1 - X/S(\partial S/\partial X)_{T,P}]$, an error which first appeared in Wilks's book.[23] Following the discovery of this error we have reanalyzed our data using the correct equation[24] to deduce ρ_s/ρ from u_2. The reanalyzed results are in good agreement with scaling and universality, removing all previous apparent contradictions. In particular we find ζ and $\rho_s l/T$ to be independent of concentration for $X \leq 0.4$.

In this paper we discuss the experimental details more extensively than was possible in our letter,[14] we present the new analysis of our data, and compare the results to theoretical predictions. In Sec. II of this paper we present the experimental apparatus and techniques used, which largely parallel those of the pure ^{4}He experiment.[7] Section III details the data acquisition and analysis, including the various checks performed during the experimental runs and data analysis. The final results are given and discussed in Sec. IV, including the Khalatnikov thermodynamic treatment of u_2 in terms of ρ_s/ρ. Our results are compared with the data of other workers and various theoretical results.

II. EXPERIMENT

A. Low-temperature apparatus

The experimental low-temperature setup is shown in Fig. 1. A vacuum can is surrounded by a pumped liquid-helium bath, which is regulated at $T_\lambda(X) - T \sim 10$ mK for each mixture. The copper sample cell filled with the mixture is suspended in the vacuum can and very weakly coupled to the bath. There are two second-sound resonators R_1 and R_2 inside the cell. A germanium thermometer[25] is potted with Apiezon N grease in a hole drilled into the copper cell. All electrical leads to the resonators pass out of the cell through epoxy-filled capillaries soldered into the cell body. The coaxial leads are heat sunk to the cell, reducing the heat introduced directly into the liquid mixture to that generated by the sound transducers.

The helium sample (about 1 cm^3) is filled through a cold valve, which is thermally anchored at the sample temperature. The valve consists of a German silver body with a 1-mm hole in it, into which a tapered stainless-steel needle fits. The needle valve is operated from room temperature. The purpose of the valve is to minimize the volume of gas above the liquid and to allow the fill line to be pumped out to reduce the heat leak into the sample. It therefore reduces variations and uncertainties in the concentration of the mixture in the sample cell, and assures that the sample is at the vapor pressure.

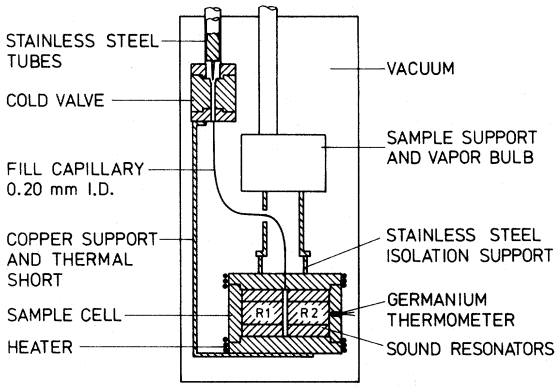

FIG. 1. Low-temperature experimental apparatus. The vacuum can shown sits in a pumped-^{4}He bath. R_1 and R_2 are the two sound resonators.

With the bath regulated to ± 0.1 mK at 10 mK below $T_\lambda(X)$, the sample could be held at temperatures near T_λ with a heat input level of about 2–4 μW. The heat was put in by a heater wound equally on the top and bottom of the sample cell.

B. Second-sound resonators

Sound was generated in two cylindrical copper cavities inside the sample cell (Fig. 1). The design and dimensions of the copper resonators are given in Fig. 2.[7] The height of the sample was kept to a

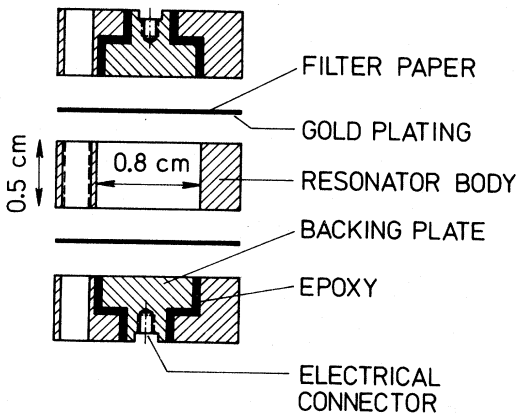

FIG. 2. Exploded cross-sectional view of sound resonator.

minimum to avoid gravity effects.[26] Each resonator was terminated at both ends by identical capacitive superleak transducers.[27] Their backing plates, serving as stationary parts of the capacitors, were mounted with electrically insulating epoxy in the end caps. The surfaces of these plates were lapped with fine sandpaper. The vibrating elements of the transducers were commercial "Nuclepore" filter membranes.[28] Membranes with two different channel diameters were used. Complete information on these membranes can be found in Ref. 7. We used GE 20 with nominal channel diameter 0.2 μm for one resonator, and GE 60 with nominal channel diameter 0.6 μm for the other resonator. Transmission micrographs indicated that the channels are quite straight and of uniform diameter over their length. Because the diameters of the "holes" are a factor of 16 and 50 smaller than the thickness of the paper (10 μm) it is more reasonable to consider them as "channels" than as "pores" or "holes." The filter membranes were plated with gold on one side to give a conducting layer with a thickness of about 300 Å. This conducting layer was electrically grounded to the resonator body. The helium sample entered the resonators by flowing through leaks between the end caps and the resonator body. The two ends of each resonator body were ground flat and mutually parallel to 0.2%. The lengths of the resonators were measured at room temperature to $\pm 5\times10^{-3}$ mm and then corrected for thermal contraction due to cooling to helium temperatures. The coaxial leads for the drive signals and for the pick-up signals were mounted in separate tubes. Plane-wave modes dominated the spectra of our resonators. The quality factor Q of the second-sound resonances, defined as the resonant frequency ν divided by the full width $\Delta\nu$ at half-power, was 1000–1500 for $T \ll T_\lambda$. It decreased with increasing temperatures to about 200 near T_λ.

C. Sound electronics

The electronic system for the sound measurements is similar to that shown in Fig. 5 of Ref. 7, and is described there. The heart of the system is a wave analyzer[29]: a band-pass filter (3-Hz bandwidth), whose center frequency is tunable, followed by an rms-voltmeter, which is used to detect the signal of the sound receiver. The analyzer also produces a sinusoidal output signal at the center frequencey of the band-pass filter for driving the sound generator. The frequency of the wave analyzer was mechanically swept at a speed of 3 Hz/sec to record the resonance spectrum of the second-sound resonators.

Both the sound generator and receiver had a bias voltage of about 240 V applied to them, so that the sound drive and detection were done at the same frequency. The generator was driven with a sinusoidal voltage of 0.695 V_{rms}. The electronic crosstalk between the drive and receiver circuits was reduced by careful shielding to about 30 nV_{rms}. However, since signals down to this level were being measured, it was important to adjust the phase of the drive to maximize the amplitude of the particular resonant harmonic used for the data analysis. The details of this procedure are discussed in Sec. III B of Ref. 7.

The signal from the receiving transducer was amplified by 60 dB before being sent to the analyzer. The analog output from the analyzer, which is proportional to the amplitude of the signal, and the frequency (after digital-to-analog conversion) were recorded on a strip-chart recorder. The frequencies and amplitudes of the resonances could be read from the recorder chart to within 1 Hz and 1% of full scale, respectively.

D. Thermometry and temperature regulation

The primary thermometer was a sealed germanium thermometer mounted in a hole in the side of the copper sample chamber. For $X=0$ through $X=0.396$ a Cryocal CR 2500 L was used, and for $X=0.555$ a Cryocal CR 1000 was used.[25] The thermometer resistance was determined using an ac-bridge circuit operated at 280 Hz with a lock-in amplifier as null detector (see Fig. 4 of Ref. 7). The bridge ratio between the strongly temperature-dependent resistance of the germanium thermometer and a very constant metal film reference resistor ($R=30$ kΩ) mounted on the sample cell was determined with a ratio transformer. The noise of this bridge circuit was about 100 nV_{rms} (with 3-sec time constant). It was possible to resolve 0.3 μK with our setup. The off-balance output from the lock-in detector was amplified and applied to a heater wound around the sample cell (see Fig. 1). This feedback loop kept the sample temperature constant to better than 1 μK. The power dissipated in the thermometer was 5×10^{-9} W, and was checked to produce no measurable self-heating effects. The bridge ratio was calibrated against the 1958 ^{4}He vapor-pressure scale, using a capacitive manometer[30] for the vapor-pressure measurements. The calculation of temperatures used a polynomial fit of the resistance R (calculated from the resistance ratio) against absolute temperature T:

$$\ln T = \sum_{i=0}^{2} A_i [\ln R]^i \quad . \tag{1}$$

E. Sample preparation

The mixtures used in this experiment were mixed at room temperature to an accuracy of $\Delta X/X = 10^{-3}$. The molar concentrations were nominally $X = 0.0$, 0.100, 0.200, 0.395, and 0.580, where the molar concentration is defined as

$$X = \frac{N_3}{N_3 + N_4} \quad . \tag{2}$$

N_3 and N_4 are the number of moles of ^{3}He and ^{4}He, respectively. The concentration of the mixtures in the sample chamber was determined from the measured $T_\lambda(X)$ and the data of Roberts and Sydoriak[31] for $T_\lambda(X)$. These concentrations were $X = 0.000$, 0.096, 0.204, 0.396, and 0.555.

The method used to fill the sample chamber avoided large changes in the concentration due to possible preferential condensation of the ^{4}He at low temperatures. A dipstick with a volume of 70 cm^3 was filled with zeolite. The dipstick was cooled to 4.2 K and about 2 STP l of the desired mixture were condensed into it. The resulting pressure in the dipstick when warmed to room temperature was 30 atm. The sample chamber was then cooled to about 1.1 K. With the sample chamber cold, the high-pressure sample gas was condensed into the sample cell and resonators through the fill capillary and the open cold valve. This effectively eliminated concentration changes during filling. After closing the cold valve, the fill line was evacuated. A small change in the concentration may have occurred, however, before the cold valve was closed since the entire fill line was filled with vapor while equilibrium was being established. Since the liquid density increases monotonically from low temperatures to T_λ,[32] closing the cold valve with a full sample cell at the lowest temperature assured that the sample would be at vapor pressure near T_λ.

III. DATA ACQUISITION AND ANALYSIS

A. Experimental procedure

The system was prepared for a run with a mixture of given concentration as described above. After preliminary λ-point determinations were made, the sample was regulated at a temperature several milli-Kelvin below T_λ. Then the acoustic system was checked by recording the resonant spectra of both resonators over a frequency range from about 100 Hz to 10 kHz. Far from T_λ the amplitudes of the second-sound resonances were, within a factor of 3, independent of concentration and transducer membrane. Resonances with high Q's were always found among the 27th to 30th harmonics, and these were then used for the data acquisition.

A careful measurement of the λ temperature was made by observing the inflection point of the first-sound velocity in the resonator equipped with the 0.2-μm membrane (see below). While the system was near T_λ where the second-sound amplitude was was very weak a phase shifter was carefully adjusted to maximize the amplitude of the harmonic to be studied (for details see Ref. 7). The system was then cooled to a temperature such that the harmonic to be studied had a received amplitude of 10–20 μV_{rms}, with a drive amplitude of 0.695 V_{rms}.

The data were acquired first in the 0.2-μm channel resonator by holding the temperature constant, and sweeping the frequency of the second sound at 3 Hz/sec through five harmonics and recording this part of the spectrum. This procedure was repeated as the temperature was increased in steps of 2–30 μK to $T_\lambda(X)$. The temperatures were established by changing the ratio transformer setting and allowing the feedback system to regulate the sample temperature. As the sound vanished it was sometimes necessary to readjust the phase of the sound drive slightly. Thermal equilibrium was always established before data were taken. This was assured by setting the wave analyzer frequency on the side of a second-sound peak where any drifts in temperature had very large effects on the observed amplitude. Once the signal was stable for 2 min, the data were recorded. An example of the results is shown in Fig. 3. The second sound is seen to vanish into the noise before T_λ is reached. For a given mixture and filter membrane the amplitude and frequency of one particular harmonic was chosen for the analysis.

After the second sound had vanished in the 0.2-μm channel resonator, the system was switched to the 0.6-μm channel resonator. In this resonator the sound persisted to higher temperatures because of the larger channel diameter of the membrane.[7] Again, starting at a temperature such that the sound amplitude was about 10 μV_{rms}, the same procedure was repeated. The entire range of ϵ covered by both sets of data is given in Table I. Following the disappearance of second sound in the 0.6-μm channels, the system was switched back to the 0.2-μm resonator for a new determination of T_λ using first sound.

B. Determination of the cutoff temperature

The disappearance of the second-sound signal indicates how far the superfluid transition had been shifted below T_λ by the restriction of the geometry for the liquid in the membrane channels. The frequency and temperature at which the sound amplitude intercepted the 0.03 μV_{rms} noise level of our system were taken as the cutoff where second

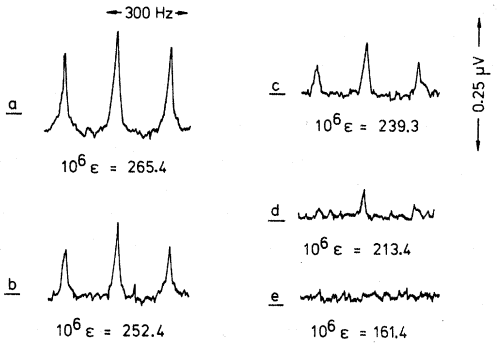

FIG. 3. Strip-chart (time) records of second-sound spectra. The sound amplitude is shown as a function of frequency, since the frequency is swept linearly in time. The spectra show harmonics $n = 28$–30 from the resonator fitted with 0.2-μm membrane and for a mixture with $X = 0.204$. The temperature has been increased in four steps going from spectrum a to spectrum c, and is given as $\epsilon = 1 - T/T_\lambda(X)$. The resonator equipped with 0.6-μm filter membrane and with the same mixture and drive amplitude showed second-sound resonance amplitudes of 9.7 μV_{rms} at the temperature of spectrum e, $10^6\epsilon = 161.4$.

sound vanished. In Sec. III C the effect of this somewhat arbitrary choice for the cutoff level will be discussed. The amplitude data were corrected by subtracting the value of the background from the peak values. The frequency of the harmonic being studied was converted to the second-sound velocity by dividing by the harmonic number and multiplying by twice the chamber length. Thus, we had a complete set of amplitude, velocity, and temperature data for each concentration and both channel sizes. The only exception is that for $X = 0.555$ we only have reliable velocity and temperature data. During this run only the resonator equipped with $d = 0.2$-μm membrane was functioning. The character of the resonance spectrum was such that we could measure the frequency interval accurately between harmonics, but could not make an accurate amplitude measurement. This was due to large overlap and interference of the harmonics. We thus could not accurately determine T_0.

Plots of second-sound amplitude versus $\epsilon = 1 - T/T_\lambda$ for each mixture are shown in Figs. 4 and 5 for $d = 0.2$ and 0.6 μm, respectively. These plots gave us a set of cutoff temperatures. For most of the runs (except for the $X = 0.396$ mixture, where the curvature was too great) it was possible to represent the amplitude A near cutoff by the equation

$$\ln(A/A_2^*) = a_2\epsilon \,. \tag{3}$$

A least-squares fit to the data established A_2^* and a_2. Putting in the cutoff amplitude A_0 for A then gave ϵ_0. Near cutoff, plots of amplitude versus frequency could also be represented by

$$\ln(A/A_1^*) = a_1\nu \,, \tag{4}$$

where ν is the sound frequency. Using A_1^* and a_1 from least-squares fits to the data, and using the cutoff amplitude gave ν_0. A graph of ν versus ϵ then gave a second value of ϵ_0. In Table II the ϵ_0 are an average of the results of the two methods.

C. Checks

The effect of varying the drive voltage applied to the sound drive transducer was investigated in mixtures with $X = 0.0$ and $X = 0.396$ for voltages of 0.695, 0.225, and 0.073 V_{rms}. It was found that the second-sound velocity was independent of these drive voltages. The intrinsic critical velocity of superfluid helium decreases strongly near the λ transition or near the temperature where superfluidity vanishes in a particular geometry.[33] If critical velocities were being reached in the filter-membrane channels of the transducers, the sound signal should probably have decreased with increasing drive voltage, owing to the reduced ef-

TABLE I. Second-sound velocity and superfluid density.

	Molar concentration of ^{3}He				
	0.000	0.096	0.204	0.396	0.555
T_λ (K)	2.171	2.032	1.863	1.518	1.167 [a]
$T_{\lambda k} - T_\lambda$ (μK)	0.6±0.5	6.6±0.5	4.9±2.5	19.6±9.0	···
ϵ range (10^{-4})	0.23–2.91	0.33–2.94	0.53–4.78	1.24–19.2	2.78–140
W	0.378	0.397	0.389	0.424	0.409
u_2^* (cm/sec)	4354	5141	4281	3704	2187
ζ	0.671	0.714	0.692	0.735	0.766
k (ζ free)	2.562	2.580	1.467	1.048	0.451
k ($\zeta = 0.672$)	2.580	1.745	1.207	0.655	0.253

[a] This value is $T_{\lambda,k}$. See text for details.

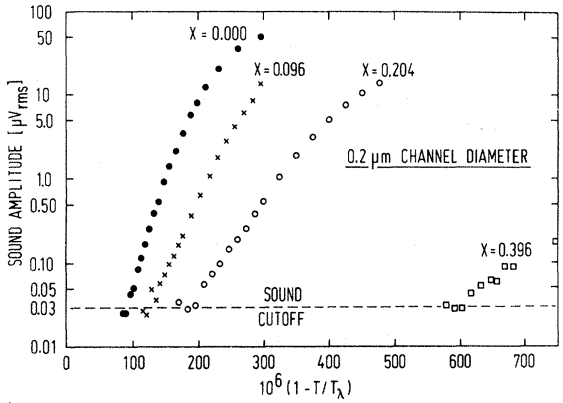

FIG. 4. Second-sound amplitude as a function of $\epsilon = 1 - T/T_\lambda(X)$ for four mixtures in the resonator equipped with 0.2-μm filter membrane. The drive voltage was 0.695 V_{rms}, and the cutoff level used for determining the reduced shift ϵ_0 of the onset temperature is indicated.

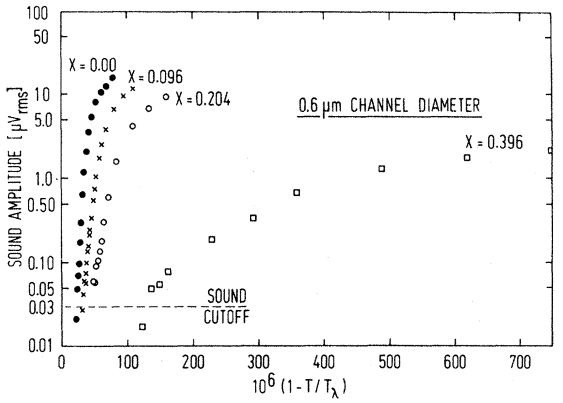

FIG. 5. Second-sound amplitude as a function of $\epsilon = 1 - T/T_\lambda(X)$ for four mixtures in the resonator equipped with 0.6-μm filter membrane. The drive voltage was 0.695 V_{rms}, and the cutoff level used for determining the reduced shift ϵ_0 of the onset temperature is indicated.

ficiency of the transducers. This would lead to a larger cutoff value ϵ_0 with increasing drive voltage since the received sound signal at a given temperature would be reduced. In fact, as can be seen in Fig. 6, the opposite was observed; each time the drive voltage was increased a factor of 3, ϵ_0 decreased by 10%. This is the same result as found for pure ^{4}He by Ihas and Pobell.[7] The cutoff temperature is thus a weak function of the drive voltage. All of our conclusions are based on data for which the sound drive was fixed at 0.695 V_{rms}. It was also determined that the heat generated by the transducers with this drive voltage was 1.5×10^{-8} W. The drive and receiver bias voltages were constant throughout the measurements.

As mentioned earlier, the cutoff level of 0.03 μV_{rms} for the second-sound amplitude is somewhat arbitrary. The absolute cutoff temperatures would be slightly different for different noise levels. To check the influence of the cutoff level on our results we carried through all the analysis concerning ϵ_0 for cutoff levels of 0.03 and 0.10 μV_{rms}. The result of increasing the cutoff level by a factor of 3.3 was to increase the values of ϵ_0 by about 15–20%. The values of $d\rho_s/T$ (see Sec. IV) were increased by about 10–15%. None of our conclusions regarding the concentration dependence of ϵ_0 or $d\rho_s/T$ are affected by the cutoff level being chosen as 0.03 μV_{rms}, or by the drive voltage being chosen as 0.695 V_{rms}.

D. Measurement of T_λ

The determination of the λ temperature for each mixture was done at the beginning and end of each run in order to check for system drifts, thermometer changes, and concentration stability. With the measured T_λ we calculated the reduced temperatures, and used Roberts and Sydoriak's[31] data for $T_\lambda(X)$ to determine the concentration of the sample.

TABLE II. Finite-size effects.

	Molar concentration of ^{3}He			
	0.000	0.096	0.204	0.396
$10^6\epsilon_0$ (for $d_1 = 0.2\ \mu$m)	91.8±0.5	128.4±4.0	193.5±4.0	603±5
$10^6\epsilon_0$ (for $d_2 = 0.6\ \mu$m)	22.5±0.1	33.1±2.0	47.1±2.7	139.4±11
$\log(\epsilon_{0,1}/\epsilon_{0,2})$	0.611	0.589	0.614	0.636
$\nu' = 1/\lambda'$	(0.672)	0.697	0.669	0.646
$10^8\, d\rho_s/T$ (g/cm^{2}K)				
(for $d = 0.2\ \mu$m)	0.653	0.585	0.557	0.700
(for $d = 0.6\ \mu$m)	0.763	0.666	0.628	0.715

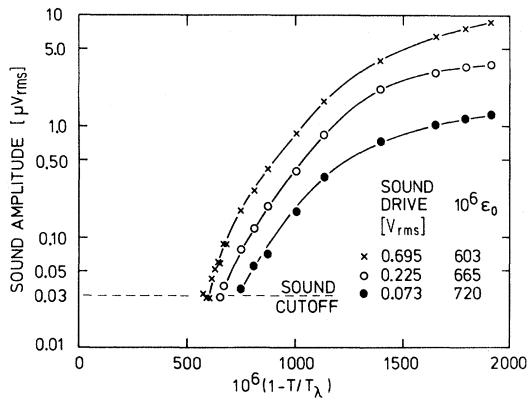

FIG. 6. Second-sound amplitude for various drive voltages as a function of $\epsilon = 1 - T/T_\lambda(X)$ in an $X = 0.396$ mixture using 0.2-μm filter membrane. The sound cutoff used for determining ϵ_0 is indicated. The inset shows the values for the weak dependence of ϵ_0 on the sound drive voltage.

The resistance of the thermometer at the λ transition was measured by observing the inflection point in the velocity of first sound as the apparatus was allowed to warm slowly (2 μK/min) through the λ point.[34,35] The first sound was generated in these resonators when the temperature was higher than that at which second sound vanishes.[7] The second sound vanished first in the 0.2-μm channels, and first sound with a quality factor $Q \simeq 500$ was generated in this resonator. Thus, this resonator was always used to measure T_λ. The system was locked in on the fundamental plane-wave mode (about 20 kHz) using the automatic frequency control mode of the wave analyzer. The first-sound frequency versus time-chart recording shows an inflection point when the liquid at the top of the sample chamber undergoes the λ transition.[34,35] The sharpness of the inflection point decreases with increasing concentration of ^{3}He. As X increases, the uncertainty in T_λ also increases. Independent checks on the measured T_λ values were obtained from least-squares fits of $u_2 = u_2^* \epsilon^W$ and $\rho_s/\rho = k\epsilon^\zeta$ as a function of ϵ with T_λ allowed to vary. These calculated values $T_{\lambda,k}$ are in excellent agreement with the measured values (see Table I for all of these data). Owing to the extremely weak specific-heat anomaly in the $X = 0.555$ mixture, no inflection point could be established. We thus relied entirely on a $T_{\lambda,k}$ determined from the u_2 and ρ_s/ρ fits for this mixture. For the other mixtures the data analysis used the measured T_λ values. The tendency of the calculated values to be higher than the measured ones is probably an artifact brought about by the narrow temperature interval over which the fits of u_2 and ρ_s/ρ were done. Within the experimental error, the λ temperatures measured at the start and at the end of a run were the same. The values of ϵ_0 for the 0.6-μm channels were much smaller than for the 0.2-μm channels, hence an accurate determination of T_λ is more important for runs with this membrane. Therefore, the value of T_λ used for the data reduction was the last one taken since it was obtained immediately after the 0.6-μm channel data.

IV. RESULTS AND DISCUSSION

A. Second-sound velocity

Second-sound measurements in the mixtures have been made by Noble and Sandiford,[17] Terui and Ikushima,[12,16] Ahlers and Greywall,[13] Uehara *et al.*,[15] and by ourselves.[14] At each concentration, the results can be fitted to the power law

$$u_2 = u_2^* \epsilon^W . \tag{5}$$

Our results for the amplitudes u_2^* and exponents W of second sound are given in Table I and in Figs. 7 and 8, respectively. The values of $u_2^*(X)$ lie close to the solid line which is a fit by Ahlers[24] to the data of Refs. 12 to 14 for $X \lesssim 0.6$. The values of the second-sound exponent obtained from our data are shown in Fig. 8 plotted as $2W$. They are seen to scatter along a smooth curve, again a fit by Ahlers[24] to the available data. The somewhat large deviation of our value for W for $X = 0.396$ is not understood at present. The values of u_2^* and W are almost independent of the concentration for values of $X \lesssim 0.2$.

B. Superfluid density

In this subsection, we will discuss the calculation of superfluid density ρ_s/ρ from the measured

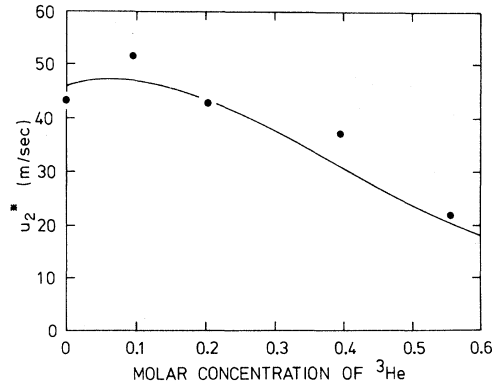

FIG. 7. Effective amplitude u_2^* of the second-sound velocity u_2 as a function of the molar ^{3}He concentration. The solid curve is a fit by Ahlers to all published data (Ref. 24).

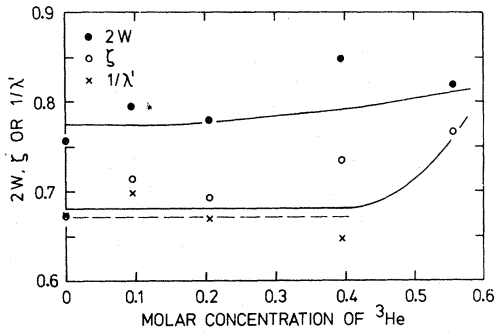

FIG. 8. Effective exponents $2W$ of u_2^2, ζ of ρ_s/ρ, and $1/\lambda'$ of $\epsilon_0=(d/d^*)^{-\lambda'}$ as a function of the molar concentration of ^{3}He. The solid curves through the data for $2W$ and ζ are fits by Ahlers to all published data (Ref. 24). The values of $1/\lambda'$ were normalized to $1/\lambda'\equiv\zeta=0.672$ at $X=0$. The dashed line is a constant, $1/\lambda'=0.671$, which is the mean value for our data.

values of the second-sound velocity and various thermodynamic parameters.[24] Incorrect conclusions regarding ρ_s/ρ which were published earlier are corrected.[14]

From two-fluid hydrodynamics Khalatnikov[18,19] obtained an expression for the second-sound velocity in mixtures in terms of the superfluid fraction ρ_s/ρ and various thermodynamic parameters. He made the assumption that the isobaric thermal expansion coefficient may be set equal to zero. His result for u_2 is

$$u_2^2=\frac{\rho_s}{\rho_n}\left[\bar{\sigma}^2\left(\frac{\partial T}{\partial\sigma}\right)_{cP}+c^2\left(\frac{\partial(Z/\rho)}{\partial c}\right)_{TP}\right](1+d)^{-1}, \tag{6}$$

where ρ_n is the normal fluid density, c is the mass concentration

$$c=\frac{N_3m_3}{N_3m_3+N_4m_4}, \tag{7}$$

where N_3 and N_4 are the number of ^{3}He and ^{4}He atoms, and m_3 and m_4 the corresponding masses of the atoms. The entropy per gram of solution is σ, and $\bar{\sigma}$ as used in Eq. (6) is

$$\bar{\sigma}=\sigma\left[1-\frac{c}{\sigma}\left(\frac{\partial\sigma}{\partial c}\right)_{TP}\right]. \tag{8}$$

By using Eq. 9.5.12 of Wilks's book[23] in our earlier calculations, we mistakenly set $\bar{\sigma}=\sigma$, as did other authors.[4,12,13,21,23] This led to our erroneous conclusions about ρ_s calculated from u_2. The quantity Z/ρ is a chemical potential difference $\mu_3^K-\mu_4^K$,[24] and

$$d=\frac{\rho_s}{\rho_n}\left[\frac{c}{\rho}\left(\frac{\partial\rho}{\partial c}\right)_{TP}\right]^2. \tag{9}$$

Since the available thermodynamic parameters are in terms of the molar concentration X, it was necessary to write Eq. (6) in terms of X instead of in terms of the mass concentration c. The result of this conversion is

$$u_2^2=\frac{M_s}{M_4^2}\left(\frac{\rho_s}{\rho_n}\right)\left[\frac{\bar{S}^2T}{C_{XP}}+X^2\left(\frac{\partial\Phi}{\partial X}\right)_{TP}\right](1+d)^{-1}, \tag{10}$$

with

$$X=\frac{N_3}{N_3+N_4}, \tag{11}$$

$$\bar{S}=S\left[1-\frac{X}{S}\left(\frac{\partial S}{\partial X}\right)_{TP}\right], \tag{12}$$

and

$$M_s=XM_3+(1-X)M_4. \tag{13}$$

M_3 and M_4 are the molar masses of ^{3}He and ^{4}He. S is the entropy per mole of solution, and C_{XP} is the specific heat per mole of solution at constant concentration. The transformation to X makes

$$d=\left(\frac{M_s}{M_4}\right)^2\left(\frac{X}{\rho}\right)^2\left(\frac{\partial\rho}{\partial X}\right)_{TP}^2\left(\frac{\rho_s}{\rho_n}\right). \tag{14}$$

Ahlers[4,24] has treated in detail the values used for the various thermodynamic parameters, and has fitted a closed-form expression for C_{XP} to the published specific heat data of Gasparini and Moldover,[36] Alvesalo *et al.*, and Islander and Zimmerman.[37] We have used the thermodynamic parameters given by Ahlers in Ref. 24. Ahlers has also shown that the assumption of a vanishing expansion coefficient gives errors in ρ_s/ρ no larger than one part in 10^3. The errors for ρ_s/ρ introduced by errors in the various parameters of Eq. (10) have also been calculated and discussed by Ahlers.

The values for ρ_s/ρ calculated from u_2 and thermodynamic parameters near T_λ were then fit to the power law

$$\rho_s/\rho=k(X)\epsilon^{\zeta(X)}. \tag{15}$$

The values of the effective exponent $\zeta(X)$ are shown in Fig. 8 as open circles and are given in Table I. The use of the correct relation between u_2 and ρ_s/ρ reduces the apparent concentration dependence of ζ obtained previously.[14] Within an uncertainty of about ±0.02, which is mainly due to uncertainties in the thermodynamic parameters, we find from our data that ζ is independent of X for $X\lesssim0.2$. The composite of all available data shows that ζ seems to be independent of X for $X\lesssim0.4$ and within the experimental error is equal to the value for pure ^{4}He.[24] The concentration independence of ζ would be in agreement with the universality concept.[2,3] However, our data would

allow a slight concentration dependence of ζ, which one also obtains from the specific heat data[36,37] via the scaling relation $\zeta = \frac{1}{3}(2 - \alpha')$. In this relation, α' is the critical exponent for the heat capacity at constant pressure. It cannot be decided from the presently available data[12-16] whether this apparent slight concentration dependence of ζ is real or is due to the rather large errors entering the analysis. If real, it may be removed by using singular higher-order correction terms in ϵ in Eq. (15). Such terms were necessary in the analysis of ρ_s/ρ in ^{4}He under pressure,[6] but the mixture data are not accurate enough to decide this question.

From the same fit, the amplitudes $k(X)$ of ρ_s/ρ were obtained, and are plotted in Fig. 9, as solid circles. In a second analysis the value of the exponent ζ was fixed at its best estimate of $\zeta = 0.672$ for pure ^{4}He.[24] The values of $k(X)$ obtained in this analysis are the open circles in Fig. 9. Both sets of values are given in Table I. The solid curve in Fig. 9 is a calculation by Ahlers[24] also based on a fixed value of $\zeta = 0.672$ and his smooth curves for u_2. The agreement between our values of $k(X)$ at each X, and Ahlers's smooth curve, indicates that $\zeta = 9.672$ is a reasonable assumption. Again, the concentration dependence of k is appreciably reduced compared to published values.[12,14,21] that were calculated using the incorrect relation between u_2 and ρ_s. The critical exponents and amplitudes of ρ_s/ρ and of u_2 are somewhat high for $X = 0.1$. We attribute this to the correlation between amplitude and exponent; the amplitude k is appreciably reduced if the exponent ζ is fixed at 0.672.

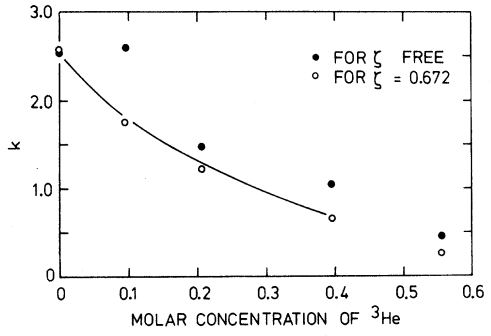

FIG. 9. Amplitude k of the superfluid fraction $\rho_s/\rho = k\epsilon^{\zeta}$ measured along a path of constant concentration as a function of the molar concentration of ^{3}He. The solid circles are from a least-squares fit, where both k and ζ were allowed to vary. The open circles are from a least-squares fit with a fixed $\zeta = 0.672$. The solid curve is calculated by Ahlers assuming that $\zeta = 0.672$ (Ref. 24).

We do not agree with the claim by Terui and Ikushima[16] that replacing S by $\bar{S}$ in deducing ρ_s/ρ from u_2 has a negligible influence on the effective exponent ζ. Their result may partly depend on the values for $S/\bar{S}$ calculated by these authors which disagree with the correct values given in Ref. 24. In addition, a revised concept of universality was discussed in Ref. 16, where critical exponents are normalized by the critical exponent ν' of the coherence length. Such a renormalization would have no influence on the question of universality because ν' is found to be independent of concentration X (see Sec. IV C) and of pressure P.[7]

C. Finite geometry effects and universality

The data discussed in Sec. III included the measurements of the temperature $T_0(X)$ at which second sound vanished in our resonators when the onset length l becomes comparable to the channel diameter in the filter membranes. From this onset temperature $T_0(X)$, we calculated the reduced temperature differences $\epsilon_0(X) = 1 - T_0(X)/T_\lambda(X)$ for each concentration and channel diameter. These data are given in Table II and plotted in Fig. 10. Whereas ϵ_0 is independent of pressure to within ±2% for ^{4}He,[7] we find a very strong concentration dependence of ϵ_0, changing by about a factor of 6 for $X = 0$ to $X = 0.4$. This is consistent with an even larger value of ϵ_0 reported in Ref. 13 for temperatures near the tricritical point. It is seen from Fig. 10 that within the errors, ϵ_0 (for $d = 0.2$ μm) $= 4\epsilon_0$ (for $d = 0.6$ μm), where d is the

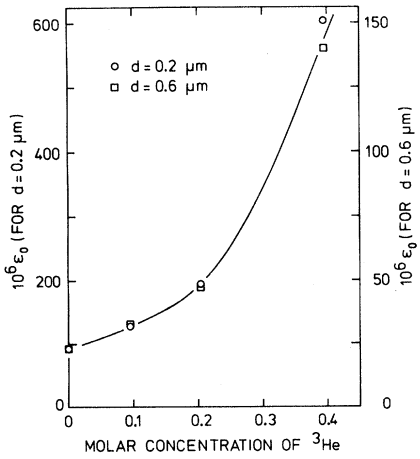

FIG. 10. Reduced shift $\epsilon_0 = 1 - T_0/T_\lambda(X)$ of the onset temperature T_0 as a function of ^{3}He concentration (using a sound cutoff of 0.03 μV_{rms}); left-hand scale: ϵ_0 measured in $d = 0.2$-μm channels; right-hand scale: ϵ_0 measured in $d = 0.6$-μm channels. The line is only a guide for the eye.

diameter of the membrane channels.

According to scaling[1] there should be only one intrinsic length describing the correlation range of singular quantities near a phase transition. This should be the bulk coherence length ξ defined in terms of the superfluid density by the relation[10,11]

$$\xi = m^2 k_B T / 4\pi\hbar^2 \rho_s = \xi^* \epsilon^{-\nu'} . \quad (16)$$

Other lengths, such as the healing length for superfluidity in channels, $l = l^* \epsilon^{-\nu'}$, should differ from this length by factors of order unity, but should have the same critical exponent.[1,4] The phenomenological Ginzburg-Pitaevskii-Mamaladze theory[38] predicts that superfluidity should vanish in a cylindrical channel of diameter d when $\xi(T_0) = 0.207d$. The reduced shift ϵ_0 is expected[20] to vary as $\epsilon_0 = (d/d^*)^{-\lambda'}$ ($d^* = \text{const}$). Therefore, λ' is proportional to $\log(\epsilon_{0,1}/\epsilon_{0,2})$, where $\epsilon_{0,i}$ is the reduced shift of the onset temperature in a channel with diameter d_i. With this equation and our data for $\epsilon_{0,i}$ in $d_1 = 0.2$-μm and $d_2 = 0.6$-μm channels we calculated the change of λ' with concentration. Since at the onset temperature the diameter d of a channel is proportional to the healing length for superfluidity, $\nu' = 1/\lambda'$. Therefore, a change of $\Delta\lambda'/\lambda'$ with concentration is identical to the behavior of $\Delta\nu'/\nu'$. We have normalized our relative values for ν' and λ' to the value $\nu' = 0.672$ for $X = 0$ to obtain absolute values (using the scaling relation $\zeta = \nu'$). The results are shown in Fig. 8 and given in Table II. Even though ϵ_0 changes drastically with concentration, the exponents λ' and ν' stay constant to within our resolution of $\pm 3\%$ for $0 \leq X \leq 0.4$, in agreement with scaling[1] and universality.[2] The concentration dependence of ϵ_0 and the concentration independence of λ' and ν' imply that the coefficients l^* and d^* as well as the healing length l at constant ϵ increase by almost a factor of 4 from $X = 0$ to 0.4.[14] In Fig. 11 we have plotted the values of

$$\frac{l^*(X)}{l^*(0)} = \left(\frac{\epsilon_0(X)}{\epsilon_0(0)}\right)^{\nu'} . \quad (17)$$

These values are an average of the results for the two-channel diameters $d = 0.2\mu$m and 0.6. Because the interatomic distance a changes only by about 7% between $X = 0$ and $X = 0.4$, the quantity l^*/a is not a constant in the mixtures.

The phase coherence length ξ given in Eq. (16) should satisfy the relation $\xi\rho_s/T = \text{const}$. If ξ and l are equal to each other except for a universal multiplicative constant, then $l\rho_s/T = \text{const}$. For pure ^{4}He this quantity was found to be independent of temperature and pressure.[7,39] Because d is proportional to l at the onset temperature, we expect

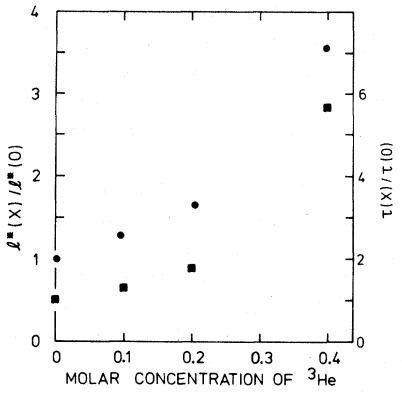

FIG. 11. Circles are the coefficient $l^*(X)$ of the onset length $l = l^* \epsilon^{-\nu'}$ as a function of the molar concentration of ^{3}He normalized to the coefficients $l^*(0)$ for pure ^{4}He. The ratios $l^*(X)/l^*(0)$ are calculated from the equation $l^*(X)/l^*(0) = [\epsilon_0(X)/\epsilon_0(0)]^{\nu'}$. The squares are the characteristic time $\tau(X) = l(X)/\mu_2(X)$ normalized to the value $\tau(0)$ for pure ^{4}He.

$$d\rho_s(\epsilon_0)/T_0 = (\text{const}) . \quad (18)$$

Using Eq. (15) for each mixture and our data for ϵ_0, we calculated $\rho_s(\epsilon_0)/\rho$ and then evaluated Eq. (18). The values of $d\rho_s/T$ at ϵ_0 are given in Table II and plotted in Fig. 12. The result that $d\rho_s/T$ for the membrane with $d = 0.2$ μm is consistently smaller than the corresponding values for $d = 0.6$ μm is identical to the results for pure ^{4}He under

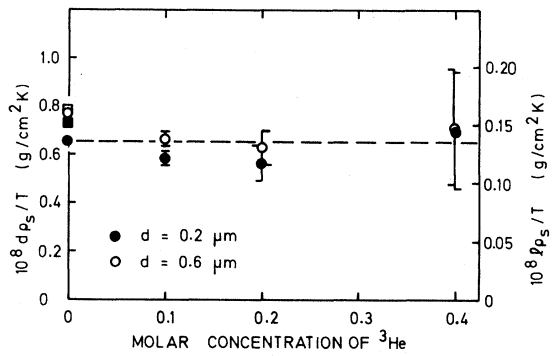

FIG. 12. Quantity $d\rho_s/T$ calculated at the onset temperature T_0 (using a sound cutoff of 0.03 μV_{rms}) for superfluidity as a function of the molar concentration of ^{3}He for $d = 0.2$-μm and $d = 0.6$-μm channels. The squares are the corresponding data of Ihas and Pobell (Ref. 7) determined at a sound cutoff of 0.1 μV_{rms}. The right-hand scale gives the same quantity with d replaced by the correlation length l calculated according to the Ginzburg-Pitaevskii-Mamaladze (Ref. 38) relation $l = 0.207d$. The error bars are those calculated by Ahlers (Ref. 24) for the uncertainty in $\rho_s(\epsilon_0)$ due to the uncertainty in the thermodynamic variables of the mixtures at T_λ. The dashed line represents the average of all our data and has the value $d\rho_s/T = 0.66 \times 10^{-8}$ g/cm^2 K.

pressure.[7] This is attributed to the actual values of d not quite agreeing with the given nominal values. The error bars in Fig. 12 are calculated by Ahlers.[24] They correspond to the uncertainty in ρ_s which arises from the uncertainty in the thermodynamic parameters. As the concentration increases, the errors get rather large. The errors in the experimental values of the cutoff temperatures give rise to an error of 1% to 10% in the calculated value for $\rho_s(\epsilon_0)$. Thus, within the combined uncertainty due to uncertainties in the value of ϵ_0 and the values of the various thermodynamic parameters we find a universal value

$$d\rho_s/T = 0.66\times10^{-8}\ \mathrm{g/cm^2\,K}. \quad (19)$$

We thus conclude that the characteristic length l determined from the onset of superfluidity in narrow channels is proportional to the phase coherence length ξ.[40]

From our data for u_2 and l we can calculate the characteristic time $\tau = l/u_2$, which is determining the attenuation of first sound in liquid helium near T_λ. We have plotted the concentration dependence of $\tau(X)$ in Fig. 12. The increase of τ with concentration is in agreement with recent results from measurements of attenuation and dispersion of first sound in ^{3}He-^{4}He mixtures.[41]

SUMMARY

We have measured the amplitude and velocity u_2 of second sound in ^{3}He-^{4}He mixtures at temperatures close to their superfluid transitions. The parameters for the equations $u_2 = u_2^* \epsilon^W$ and $\rho_s/\rho = k\epsilon^\zeta$ for $X \leq 0.555$ have been determined. Within our errors the effective exponent ζ is found to be independent of the concentration for $X < 0.4$ in agreement with predictions based on scaling and univervality.

Measuring the amplitudes of the second-sound signals we have determined the onset temperature $T_0(X)$ for superfluidity in the mixtures. The onset temperatures were determined in channels of $d = 0.2$-μm and $d = 0.6$-μm diameters. The reduced shift $\epsilon_0 = 1 - T_0(X)/T_\lambda(X)$ shows a strong concentration dependence. The exponents for the equations $\epsilon_0 = (d/d^*)^{-\lambda'}$ and $l = l^* \epsilon^{-\nu'}$ are independent of concentration to within $\pm 3\%$ for $X \leq 0.4$ in agreement with the universality concept (l is the superfluid healing length). The quantity $l\rho_s/T$ measured at ϵ_0 is found to be independent of concentration. We conclude that the healing length l in the mixtures is proportional to the phase coherence length ξ.

ACKNOWLEDGMENTS

We are grateful to G. Ahlers for many discussions and for his help during the data analysis. We thank C. Buchal for assistance with the data analysis. This work was supported in part by the Deutsche Forschungsgemeinschaft.

---

*Present address: Physics Department, Brookhaven National Laboratory, Upton, N. Y. 11973.

†Present address: Physics Department, Ohio State University, Columbus, Ohio 43210.

[1] B. Widom, J. Chem. Phys. 43, 3892 (1965); 43, 3898 (1965); L. P. Kadanoff, Physics (N.Y.) 2, 263 (1966); R. B. Griffiths, Phys. Rev. 158, 176 (1967).

[2] L. P. Kadanoff, in *Proceedings of the International School of Physics "Enrico Fermi" Course LI*, edited by M. S. Green (Academic, New York, 1973); R. B. Griffiths, Phys. Rev. Lett. 24, 1479 (1970).

[3] K. G. Wilson and M. E. Fisher, Phys. Rev. Lett. 28, 240 (1972); K. G. Wilson, *ibid.* 28, 548 (1972); E. Brézin, D. J. Wallace, and K. G. Wilson, *ibid.* 29, 591 (1972); Phys. Rev. B 7, 232 (1973).

[4] G. Ahlers, in *The Physics of Liquid and Solid Helium*, edited by J. B. Ketterson and K. H. Bennemann (Wiley, New York, to be published), Vol. 1.

[5] F. Pobell, Proc. of the Israel Physical Soc. (to be published).

[6] D. S. Greywall and G. Ahlers, Phys. Rev. Lett. 28, 1251 (1972); Phys. Rev. A 7, 2145 (1973).

[7] G. G. Ihas and F. Pobell, Phys. Rev. A 9, 1278 (1974).

[8] G. Ahlers, Phys. Rev. A 8, 530 (1973).

[9] K. H. Mueller, F. Pobell, and G. Ahlers, Phys. Rev. Lett. 34, 513 (1975).

[10] R. A. Ferrell, N. Menyhárd, H. Schmidt, F. Schwabl, and P. Szépfalusy, Ann. Phys. (N.Y.) 47, 565 (1968); B. I. Halperin and P. C. Hohenberg, Phys. Rev. 117, 952 (1969).

[11] M. E. Fisher, M. N. Barber, and D. Jasnow, Phys. Rev. A 8, 1111 (1973).

[12] G. Terui and A. Ikushima, Phys. Lett. A 43, 255 (1973); A. Ikushima and G. Terui, Phys. Lett. A 47, 387 (1974).

[13] G. Ahlers and D. S. Greywall, Phys. Rev. Lett. 29, 849 (1972); and in *Proceedings of the Thirteenth International Conference on Low Temperature Physics*, Boulder, Colo., 1972, edited by W. J. O'Sullivan *et al.* (Plenum, New York, 1973).

[14] W. C. Thomlinson, G. G. Ihas, and F. Pobell, Phys. Rev. Lett. 31, 1284 (1973).

[15] F. Uehara, T. Kobayashi, A. Tominaga, and Y. Narahara, Phys. Lett. A 50, 83 (1974).

[16] G. Terui and A. Ikushima, J. Low Temp. Phys. 16, 291 (1974); and unpublished.

[17] S. M. Noble and D. J. Sandiford, J. Phys. C 3, L123 (1970).

[18] I. M. Khalatnikov, Zh. Eksp. Teor. Fiz. 23, 169 (1952); 23, 265 (1952); and Usp. Fiz. Nauk 60, 69 (1956).

[19] I. M. Khalatnikov, *Theory of Superfluidity* (Benjamin,

New York, 1965).
[20]A. E. Ferdinand and M. E. Fisher, Phys. Rev. 185, 832 (1969); M. A. Moore, Phys. Lett. A 37, 345 (1971); M. E. Fisher and M. N. Barber, Phys. Rev. Lett. 28, 1516 (1972).
[21]G. Ahlers, Phys. Lett. A 46, 89 (1973).
[22]This error was originally pointed out to us by G. Ahlers.
[23]J. Wilks, *The Properties of Liquid and Solid Helium* (Clarendon, Oxford, 1967), Eq. 9.5.12.
[24]G. Ahlers, Phys. Rev. A 10, 1670 (1974).
[25]Cryo Cal Inc., Riviera Beach, Fla.
[26]G. Ahlers, Phys. Rev. 171, 275 (1968).
[27]R. Williams, S. E. A. Beaver, J. C. Fraser, R. S. Kagiwada, and I. Rudnick, Phys. Rev. Lett. A 29, 279 (1969); R. A. Sherlock and D. O. Edwards, Rev. Sci. Instrum. 41, 1603 (1970).
[28]Nuclepore Corp., 7035 Commerce Circle, Pleasanton, Calif. Information on the membranes was supplied by S. C. Furman.
[29]Model 1900-A, General Radio Corp., Concord, Mass.
[30]Barocel 511-11, CGS Datametrics, Watertown, Mass.
[31]T. R. Roberts and S. G. Sydoriak, Phys. Fluids 3, 895 (1960).
[32]E. C. Kerr, Phys. Rev. Lett. 12, 185 (1964).
[33]J. R. Clow and J. D. Reppy, Phys. Rev. Lett. 19, 291 (1967).
[34]G. Ahlers, Phys. Rev. 182, 352 (1969).
[35]W. C. Thomlinson and F. Pobell, Phys. Rev. Lett. 31, 283 (1973).
[36]F. Gasparini and M. R. Moldover, Phys. Rev. Lett. 23, 749 (1969); F. M. Gasparini, Ph. D. thesis (Univ. of Minnesota, 1970) (unpublished).
[37]T. A. Alvesalo, P. M. Berglund, S. T. Islander, G. R. Pickett, and W. Zimmermann, Jr., Phys. Rev. A 4, 2354 (1971); S. T. Islander and W. Zimmermann, Jr., *ibid.* 7, 188 (1973).
[38]V. L. Ginzburg and L. P. Pitaevskii, Zh. Eksp. Teor. Fiz. 34, 1240 (1958) [Sov. Phys.–JETP 7, 858 (1958)]; Yu. G. Mamaladze, Zh. Eksp. Teor. Fiz. 52, 729 (1967) [Sov. Phys.–JETP 25, 479 (1967)].
[39]I. Rudnick and J. C. Fraser, J. Low Temp. Phys. 3, 225 (1970); E. S. Sabisky and C. H. Anderson, Phys. Rev. Lett. 30, 1122 (1973).
[40]Our earlier conclusion (Ref. 14) that $d\rho_s/T$ is concentration dependent resulted from the wrong values of ρ_s, which were due to the use of S instead of $\bar{S}$ in the relation between u_2 and ρ_s (see Sec. IV B).
[41]C. Buchal, F. Pobell, and W. C. Thomlinson, Phys. Lett. A 51, 19 (1975).